Yeast
Yeast 2011; **28**: 293–308.
Published online 12 January 2011 in Wiley Online Library
(wileyonlinelibrary.com) **DOI:** 10.1002/yea.1839

Research Article

Candida albicans Tpk1p and Tpk2p isoforms differentially regulate pseudohyphal development, biofilm structure, cell aggregation and adhesins expression

Romina Giacometti[1], Florencia Kronberg[1], Ricardo M. Biondi[2] and Susana Passeron[1]*
[1]*Cátedra de Microbiología, Facultad de Agronomía, Universidad de Buenos Aires, INBA-CONICET, Avda. San Martín 4453, C1417DSE Buenos Aires, Argentina*
[2]*Research Group PhosphoSites, Medizinische Klinik I, Universitätsklinikum Frankfurt, Theodor-Stern-Kai 7, 60590 Frankfurt, Germany*

**Correspondence to: Susana Passeron, Cátedra de Microbiología, Facultad de Agronomía, Universidad de Buenos Aires, INBA-CONICET, Avda. San Martín 4453, C1417DSE Buenos Aires, Argentina. E-mail: passeron@agro.uba.ar*

Received: 28 December 2009
Accepted: 26 November 2010

Abstract

Candida albicans **undergoes a reversible morphological transition from single yeast cells to pseudohyphal and hyphal filaments. In this organism, cAMP-dependent protein kinase (PKA), coded by two catalytic subunits (*TPK1* and *TPK2*) and one regulatory subunit (*BCY1*), mediates basic cellular processes, such as the yeast-to-hypha transition and cell cycle regulation. It is known that both Tpk isoforms play positive roles in vegetative growth and filamentation, although distinct roles have been found in virulence, stress response and glycogen storage. However, little is known regarding the participation of Tpk1p and/or Tpk2p in pseudohyphal development. This point was addressed using several *C. albicans* PKA mutants having heterozygous or homozygous deletions of *TPK1* and/or *TPK2* in different *BCY1* genetic backgrounds. We observed that under hypha-only inducing conditions, all *BCY1* heterozygous strains shifted growth toward pseudohyphal morphology; however, the pseudohypha : hypha ratio was higher in strains devoid of *TPK2*. Under pseudohypha-only inducing conditions, strains lacking *TPK2* were prone to develop short and branched pseudohyphae. In *tpk2* Δ/*tpk2* Δ strains, biofilm architecture was markedly less dense, composed of short pseudohyphae and blastospores with reduced adhesion ability to abiotic material, suggesting a significant defect in cell adherence. Immunolabelling assays showed a decreased expression of adhesins Als1p and Als3p only in the *tpk2* Δ/*tpk2* Δ strain. Complementation of this mutant with a wild-type copy of *TPK2* restored all the altered functions: pseudohyphae elongation, biofilm composition, cell aggregation and adhesins expression. Our study suggests that the Tpk2p isoform may be part of a mechanism underlying not only polarized pseudohyphal morphogenesis but also cell adherence. Copyright © 2011 John Wiley & Sons, Ltd.**

Keywords: ***Candida albicans*****; PKA; pseudohyphal development; biofilm architecture; adhesins**

Introduction

Candida albicans is a pathogenic fungus that exists in multiple cell forms, including yeast, pseudohyphae and hyphae. Although pseudohyphae superficially resemble true hyphae, it is becoming increasingly clear that there are fundamental differences between the two forms in the organization of the cell cycle and the septin cytoskeleton (Sudbery et *al*., 2004). Pseudohyphal cells are highly branched, ellipsoidal in form and have constrictions at cell junctions where hyphal cells

have parallel sides and lack constrictions at their septa. Other differences include nuclear division and the presence of a specialized structure only present in hyphal cells, the Spitzenkörper, which is important for concentrating and delivering secretory vesicles to the cell tip (Braun *et al.*, 2000; James *et al.*, 2006). Because of the extensive phenotypic differences between hyphal and pseudohyphal cells, it is generally believed that expression of different gene sets specifies the morphology, although definitive evidence for this is lacking. *C. albicans* yeast cells can be induced to form hyphae or pseudohyphae by a variety of environmental signals, such as the presence of serum, 35–37 °C growth temperature and neutral pH (Odds, 1988; Sudbery, 2001). Although the mechanism underlying pseudohyphae formation is still unknown, several authors have identified specific proteins involved in the process (Li *et al.*, 2006; Sherwood and Bennett, 2008; Trunk *et al.* 2009). A recent report by Carlisle *et al.* (2009) demonstrated a continuous transition from yeast to pseudohyphae to hyphae, controlled by the dosage-dependent expression of a filament-specific transcriptional regulator, Ume6p.

In *C. albicans*, the cAMP/cAMP-dependent protein kinase (PKA) pathway mediates basic cellular processes, including dimorphic transitions. Positive roles have been established for both catalytic isoforms Tpk1p and Tpk2p in hyphae formation (Bockmühl *et al.*, 2001; Cloutier *et al.*, 2003). Jung and Stateva (2003) have demonstrated that in liquid media, constitutive activation of the cAMP pathway following deletion of *PDE2*, encoding the high cAMP-affinity phosphodiesterase, inhibits hyphal but not pseudohyphal growth. In addition, it was reported that overexpression of the transcription factor *EFG1* results in a pseudohyphal growth form rather than true hyphae (Stoldt *et al.*, 1997; Tebarth *et al.*, 2003). More recently, we have shown that heterozygous strains for the regulatory subunit of PKA (*BCY1*) in a wild-type and in a null *TPK2* genetic background promote pseudohyphal growth in several true hyphae-inducing liquid media (Giacometti *et al.*, 2006). In this work, we investigated pseudohyphal development of several PKA mutants having heterozygous or homozygous deletions of *TPK1* and/or *TPK2* in different *BCY1* genetic backgrounds. We provide genetic evidence that deletion of *TPK2* but not *TPK1* upholds pseudohyphal growth under true hyphae-inducing conditions. Under pseudohyphae-inducing conditions, *tpk2* Δ/*tpk2* Δ strains were severely impaired in pseudohypha extension. We also show that in these strains biofilm architecture is structurally weakened. Immunolabelled hyphae indicated that expression of adhesins Als1p and Als3p is diminished in the *tpk2* Δ/*tpk2* Δ mutant in comparison with the *tpk1* Δ/*tpk1* Δ strain. Our work shows that, although not required for initial germ-tube formation, Tpk2p is necessary for pseudohypha extension. Furthermore, our data indicate that Tpk2p plays an important role in biofilm formation and cell adhesion to various supports, including silicone surfaces used in medical devices.

Materials and methods

Chemicals

Reagents were obtained from the following sources: calcofluor white (CFW) and kemptide (LRRASLG) were from Sigma; phosphocellulose paper P-81 was from Whatman; [^{32}P]ATP and [^{3}H]cAMP were from New England Nuclear; polyvinylidenedifluoride (PVDF) membranes (Immobilon-P) were from Millipore; MDY4-64, Alexa Fluor 488 and concanavalin A (Alexa Fluor 594) were from Molecular Probes–Invitrogen; all restriction enzymes used were from Promega; 'Complete Mini' protease mix was from Roche. All other chemicals were of analytical grade.

Strains, media, and culture conditions

We performed the studies with new and previously obtained *C. albicans* PKA mutant strains, all derived from the wild-type strain CAI4, as detailed in Table 1. Yeast cells were cultured at 30 °C in YPD (1% yeast extract, 2% peptone, and 2% dextrose) or in SD minimal medium (Sherman *et al.*, 1986).

In all strains used in this study, the *URA3* gene was re-established with the CIp10 vector (Murad *et al.*, 2000), ensuring *URA3* expression at the neutral *RPS10* locus.

Heat stress sensitivity test

Sensitivity to heat shock was assessed as previously described (Giacometti *et al.*, 2009). Briefly, cells of wild-type and PKA mutants from the stationary

DOI: 10.1002/yea

Table 1. *C. albicans* strains used in this study

Strain	Genotype	Source or reference
CAI4	*ura3*::λ*imm434*/*ura3*:: λ*imm434*	Fonzi and Irwin, 1993
RGI4	Same as CAI4 but *RPS10*/*rps10*Δ::Clp10	Giacometti *et al*., 2009
RG65	Same as CAI4 but *BCY1*/*bcy1*Δ::*Cat* *RPS10*/*rps10*Δ::Clp10	Giacometti *et al*., 2009
RG11.1	Same as CAI4 but *BCY1*/*bcy1*Δ::*Cat TPK1*/*tpk1*Δ *RPS10*/*rps10*Δ::Clp10	This study
R1U1.1	Same as CAI4 but *TPK1*/*tpk1*Δ *RPS10*/*rps10*Δ::Clp10	This study
IIHH6-4a	Same as CAI4 but *tpk1*Δ::*hisG*/*tpk1*Δ::*hisG*	Bockmühl *et al*., 2001
RS1u	Same as IIHH6-4a but *RPS10*/*rps10*Δ::Clp10	Giacometti *et al*., 2009
RG12	Same as IIHH6-4a but *BCY1*/*bcy1*Δ::*URA3-dpl200*	This study
RG12.1u	Same as RG12 but *BCY1*/*bcy1*Δ::*dpl200* *RPS10*/*rps10*Δ::Clp10	This study
R2U2.1	Same as CAI4 but *TPK2*/*tpk2*Δ *RPS10*/*rps10*Δ::Clp10	This study
RS2u	Same as CAI4 but *tpk2*Δ::*Cat*/*tpk2*Δ::*Cat* *RPS10*/*rps10*Δ::Clp10	Giacometti *et al*., 2009
RS11u	Same as CAI4 but *tpk2*Δ::*hisG*/*tpk2*Δ::*hisG TPK1*/*tpk1*Δ::*hisG RPS10*/*rps10*Δ::Clp10	Giacometti *et al*., 2009
BBA1u	Same as CAI4 but *tpk2*Δ::*Cat*/*tpk2*Δ::*Cat* *BCY1*/*bcy1*Δ *RPS10*/*rps10*Δ::Clp10	This study
EC1u	Same as CAI4 but *tpk2*Δ::*Cat*/*tpk2*Δ::*Cat* *bcy1*Δ::*Cat*/*bcy1*Δ::*Cat RPS10*/*rps10*Δ::Clp10	This study
HPY421	*tpk2*Δ::*hisG*/*tpk2*Δ::*hisG*::*TPK2*-dpl200 *ura3*Δ::*imm434*/*ura3*Δ::*imm434*::*URA3*	Park *et al*., 2005
HPY321	*tpk1*Δ::*hisG*/*tpk1*Δ::*hisG*::*TPK1*-dpl200 *ura3*Δ::*imm434*/*ura3*Δ::*imm434*::*URA3*	Park *et al*., 2005

phase were streaked out on YPD plates and incubated at 50 °C for 30 min, 1 h and 2 h. At these time points, the plates were shifted to 30 °C and growth was analysed after 2 days.

Filamentation assays

C. albicans inoculated from a freshly grown YPD plate was cultured for 16 h at 30 °C in liquid YPD, at which point the culture was 95% unbudded and the cell density was 2×10^8 cells/ml. To promote hypha-only formation, the culture was diluted (to 1×10^7 cells/ml) with pre-warmed liquid YPD medium (37 °C) supplemented with 10% FBS or in pre-warmed minimal medium (37 °C) containing 10 mM GlcNAc (Shepherd *et al*.,1980). The cells were then cultured at 37 °C. Alternatively, to promote pseudohypha-only formation, the cells were incubated in liquid YPD at 35 °C (Sudbery, 2001). Chitin staining was done by directly adding 1 μg calcofluor white (CFW) to 100 μl of cell suspension, followed by 15 min incubation and washing. Vacuoles were stained with the lipophylic dye MDY4-64 (Cole *et al*., 1998). Nuclei were stained with DAPI. The cells were visualized with an Olympus BX50 fluorescence microscope. Images were taken with a Cool SNAP-Pro colour digital camera kit with Image Pro Plus software (Media Cybernetics).

Anti-Als immunolabelling of cultured germ tubes

The experiments were performed essentially as described by Coleman *et al*., (2009). Solid YPD cultures were stored at 4 °C for no more than 1 week before a fresh plate was prepared. Starter cultures were grown to saturation by inoculating a single colony into 10 ml YPD liquid medium and incubating for 16 h at 30 °C. For germ tube assays, yeast cells from the saturated starter culture were washed with phosphate-buffered saline (PBS) and suspended at a density of 5×10^6 cells/ml in pre-warmed YPD plus 10% fetal bovine serum (FBS). At various time points, cells were harvested by filtration through a 0.22 μm pore size filter and fixed in 3% paraformaldehyde. Fixed *C. albicans* cells were washed three times with PBS prior to and between each step in the immunolabelling protocol. Cells were resuspended in 15 μl/ml normal goat serum for 15 min at room temperature to block non-specific antibody binding. The cells were incubated in 18 μg/ml anti-Als1 and anti-Als3 monoclonal antibodies in PBS for 60 min at 4 °C on a rotating mixer and then in 3 μg/ml Alexa Fluor

DOI: 10.1002/yea

Table 2. Primers used in this study

Name	Sense	Sequence 5′ → 3′
BCY1KO5	Forward	CTAAAGTAAGTAAATGAGTGAGAGGGAGAGACAGAGA GCGAGAGGGGGAGTAAAAGTTTTCCCAGTCACGACGTT
BCY1KO3	Reverse	TCGCAACGAAAACACCAGAAAGTGAGTAAGCCAAAAA AAAAAAGATAGAATATACTGTGGAATTGTGAGCGGATA
URA3ver5	Forward	TTCCGAGCTTGGCGTAATCAT
BCY1ver3	Reverse	GGAAAGCAAAAAGTGTAAACAA
RT1-BCY1	Forward	ATGTCTAATCCTCAACAACA
RT2-BCY1	Reverse	TTAATGACCAGCAGTTGG
RT1-TPK1	Forward	AGAAGTTCAAGATGTGACTTAT
RT2-TPK1	Reverse	ACAAGGTGGTTCTGATGATG
RT1-TPK2	Forward	GAAGTTAGTACCGTTACATGG
RT2-TPK2	Reverse	ACTGCTGATTTGACAAGAAG
RT1-ACT1	Forward	CCCAAGCTTGCCGGTGACGACGCT
RT2-ACT1	Reverse	GTGGTGAACAAATGGATGGACCA

488-conjugated donkey anti-mouse IgG under the same conditions. Wet mounts of immunolabelled cells were examined using an Olympus FV300 confocal scanning laser microscope with a fluorescein isothiocyanate protocol and with excitation at 488 nm (Argon laser). The lenses used included Zeiss UplanFI 20x/0.5 and UplanApo 40x/1.0 water immersion objectives. Images were captured and processed using Photoshop v 5.5 software (Adobe Systems, San Jose, CA, USA).

DNA manipulations

DNA purifications were performed with Qiagen affinity columns, following the manufacturer's recommendations. Bacterial plasmid DNA was isolated by the alkaline lysis method (Sambrook *et al*., 1989) or using the QIAprep Spin Miniprep Kit (Qiagen). Yeast genomic DNA was isolated according to Adams *et al*. (1997). DNA modifying enzymes were used according to the manufacturers' recommendations.

Generation of *C. albicans tpk1 Δ/tpk1 Δ BCY1/bcy1 Δ* mutant strain

Knockout of one allele of the *BCY1* gene was generated using the PCR-based adaptation (Wilson *et al*., 1999) of the sequential URA-Blaster technique (Fonzi and Irwin, 1993), as previously described in Giacometti *et al*. (2009). Specific primers BCY1KO5 and BCY1KO3 were designed to generate the PCR deletion construct *BCY1::dpl200-URA3-dpl200*. The products of 10 PCR reactions were pooled and used to transform CAI4-derived strain *tpk1 Δ/tpk1 Δ* (IIHH6-4a), following the protocol described by Wilson *et al*. (1999). This technique allowed us to obtain strain *tpk1 Δ/tpk1 Δ BCY1/bcy1 Δ* (RG12). *URA3* transformants were grown on uridine-deficient SD solid medium, and proper genomic insertion of the transforming cassette was determined by a PCR-based analysis of transformed colonies, using a set of primers combining a forward oligo internal to the *URA3* cassette (URA3ver5) and a reverse one external to the modified region (BCY1ver3). From 21 independent isolations for mutant *tpk1 Δ/tpk1 Δ BCY1/bcy1 Δ*, 13 colonies showed heterozygous loss of the *BCY1* allele. Three *tpk1 Δ/tpk1 Δ BCY1/bcy1 Δ* clones rendered identical phenotypes in the characterization assays. All primers used are detailed in Table 2.

To evaluate whether *URA3* prototrophy located in the modified gene of interest affected the observed phenotypes, we performed all tests in the entire set of mutants expressing *URA3* at the neutral *RPS10* locus. To that end, the *URA3* marker was recycled by selection on SD medium plus 5-FOA (1 mg/ml) and uridine (50 μg/ml), and all *ura3* mutants were transformed with *Stu*I-digested CIp10 plasmid (Murad *et al*., 2000) in order to avoid potential problems associated with ectopic expression of *URA3* (Brand *et al*., 2004).

Preparation of cell extracts and enzymatic assays

Yeast cells ($1–2 \times 10^7$) from stationary phase were suspended in 500 μl 10 mM sodium phosphate

DOI: 10.1002/yea

buffer, pH 6.8, containing 1 mM EGTA, 1 mM EDTA, 10 mM 2-mercaptoethanol and one tablet of 'Complete mini' protease mix per 10 ml. All manipulations were thereafter performed at 4 °C. Cells were lysed by disruption with glass beads as described previously (Cassola *et al*., 2004). The resulting suspension was spun down in a microfuge at maximum speed for 30 min and the supernatant was centrifuged for 45 min at $100\,000 \times g$. This second supernatant was used immediately for enzymatic assays. PKA activity was measured as previously described (Giacometti *et al*., 2009), using [γ^{32}P]ATP as the phosphate donor. PKA-specific activity was expressed as pM ^{32}P incorporated to kemptide per min and per mg of protein. The reactions were carried out under conditions of linearity with respect to the amount of extract and the time of incubation.

cAMP binding measurements were performed as previously described (Zelada *et al*., 1998). Samples were incubated at 28 °C for 30 min in a final volume of 50 µl containing 15 mM Tris–HCl, pH 7.5, 7 mM $MgCl_2$, 1.4 mM 2-mercaptoethanol, 600 mM NaCl and 210 nM [^{3}H]cAMP (250.000 dpm). The reaction was terminated by filtering the samples through 0.45 µm nitrocellulose membranes. Non-specific binding was determined in the presence of 100 µM cAMP.

Protein determination

Protein concentration was determined by the method of Lowry *et al*. (1951) using bovine serum albumin as standard.

Western blot analysis

Bcy1p expression was assessed by Western blot. Proteins from soluble extracts were resolved by 10% SDS–PAGE, transferred to PVDF membranes, which were blocked with 5% non-fat dried milk and incubated overnight with anti-*C. albicans* Bcy1 antiserum generated in the laboratory. Immunological detection was performed using anti-rabbit IgG conjugated to alkaline phosphatase. For Bcy1p expression level, analysis loading and transfer were monitored by Ponceau S staining of the membranes. Pre-stained carbonic anhydrase was also included as a loading control.

RNA isolation and semi-quantitative RT–PCR

Total RNA was isolated from stationary growth cells by the hot-phenol method (Ausubel *et al*., 1994). Isolated RNA was then treated with DNase at 37 °C for 30 min. The SuperScript First-Strand Synthesis System kit for RT–PCR (Invitrogen) was then used to synthesize cDNA. RNA concentration was measured spectrophotometrically and 2 µg were added to the cDNA synthesis reaction. OligodT (Invitrogen) was used to prime the cDNA synthesis reaction. One-tenth volume of the final cDNA product was added to PCR reactions specific for each gene. Primer sequences for *BCY1* (RT1-BCY1 and RT2-BCY1), *TPK1* (RT1-TPK1 and RT2-TPK1) and *TPK2* (RT1-TPK2 and RT2-TPK2) are detailed in Table 2. Samples were denatured at 94 °C for 2 min, followed by 15–30 cycles of (94 °C for 45 s, 55 °C for 45 s and 72 °C for 30 s). The levels of amplified products were determined at several cycle intervals to ensure that samples were analysed during the exponential phase of amplification. We performed reactions without reverse transcriptase to control for the presence of contaminating DNA. A 900 bp PCR product amplified with RT1-ACT1 and RT2-ACT1 primers from *C. albicans ACT1* was used as internal mRNA loading control. Transcripts were quantified using ImageJ (Abramoff *et al*., 2004).

Biofilm formation

Development of biofilms was performed using a modification of a protocol described by Chandra *et al*. (2001). Briefly, *C. albicans* strains were grown in SD medium plus 50 mM glucose, pH 7.0, at 30 °C for 16 h with orbital agitation. Cells were then centrifuged and resuspended in PBS to $OD_{595} = 1.0$ and 100 µl of cells were allowed to adhere for 90 min at 37 °C to wells of a sterile 96-well polystyrene microtitre plate (Falcon) coated with 10% FBS. Cells that did not adhere were removed by washing twice with 200 µl PBS. SD medium supplemented with glucose was then added to each well and the biofilms allowed to form at 37 °C for up to 48 h.

For crystal violet staining, each well was washed twice with PBS, dried for 1 h at room temperature and stained with 110 µl 0.4% aqueous crystal violet solution for 45 min. The wells were then washed four times with 200 µl MilliQ sterile water and destained with 200 µl 95% ethanol. After

DOI: 10.1002/yea

45 min, 100 μl destaining solution was withdrawn from each well and transferred to a new plate that was measured with a microtitre plate reader (Multiskan MS, Labsystems, Finland) at 540 nm. The absorbance values of the controls were subtracted from the values of the test wells to minimize background interference. Three independent experiments were performed with 10 replicates for each strain.

For the XTT reduction assay, an XTT solution was prepared (1 mg/ml in PBS) and filter-sterilized through a 0.22 μm pore size filter. Menadione solution (0.4 mM in acetone) was filtered and mixed with XTT solution at a ratio of 1 : 5 by volume before the assay. After biofilm formation, the wells were washed three times with 200 μl PBS. To each well, 200 μl PBS and 12 μl XTT–menadione solution were added. The culture plate was incubated in the dark for 2 h at 37 °C, then 100 μl of each sample were transferred to a new plate and measured with a microtitre plate reader at 492 nm. The absorbance values of the controls were subtracted from the values of the test. The experiment was performed three times, using 10 replicates for each strain.

To analyse the adhesion and biofilm formation of *C. albicans* strains to a relevant medical device, we evaluated the ability of strains to adhere and form biofilms on a catheter silicone surface. In this experiment, the strains were grown overnight in YPD at 30 °C, diluted to $OD_{600} = 0.5$ in 2 ml Spider medium (Liu *et al*., 1994) and added to a sterile 12-well plate containing a silicone elastomer square, pretreated overnight with 10% FBS. The inoculated plate was incubated at 37 °C for 90 min with shaking to allow the initial adhesion of cells. The squares were washed with 2 ml PBS and placed into 12-well plates containing 2 ml fresh Spider medium and incubated at 37 °C for an additional 48 h to allow biofilm formation. The biofilm mass on the silicone substrate was observed by concanavalin A staining, as described by Kuhn *et al*. (2002). Cells were visualized with an Olympus FV300 confocal scanning laser microscope with a rhodamine-fluorescein isothiocyanate protocol [excitation at 543 nm (HeNe laser) and emission at 560 nm]. The lenses used included Zeiss UplanFI ×20/0.5 and UplanApo ×40/1.0 water immersion objectives. Images were captured and processed using Photoshop v 5.5 software.

Measurement of pseudohyphal length and constrictions

Quantitative cell measurements of microscopic images were made using ImageJA version 1.42I software. The average diameters and the intersepta distances were determined from measurements of CFW stained cells; more than 200 individual pseudohyphal filaments per strain were measured. Pseudohyphal lengths and diameters were traced directly from images and constriction frequency was measured by assessing: (a) the average numbers of compartments from the pseudohyphal apex to the first constriction; and (b) the percentage of subapical pseudohyphal compartments that had a branch or lateral bud.

Results and discussion

Absence of Tpk2p isoform enriched pseudohyphae population under hypha-only inducing conditions

Previous work from our laboratory showed that strains lacking a *BCY1* allele in a wild-type and in *TPK2* null genetic background exhibited a mixture of true hyphae and pseudohyphae in several liquid inducing media (Giacometti *et al*., 2006). Therefore, it seemed relevant to examine the germinative phenotype of a heterozygous *BCY1* mutant in a background devoid of *TPK1* isoform, since a recent report from our laboratory showed that Tpk1p and Tpk2p isoforms have distinct roles in the stress response pathway and in glycogen accumulation (Giacometti *et al*., 2009).

With this in mind, we performed the heterozygous disruption of *C. albicans BCY1* in the strain *tpk1* Δ*/tpk1* Δ (see Material and methods). The phenotype and biochemical characteristics of the *tpk1* Δ*/tpk1* Δ *BCY1/bcy1* Δ (RG12.1u) strain are summarized in Table 3 and Figure 1. PKA activity was routinely measured at the stationary phase because levels of *TPK1* and *TPK2* mRNA expression are at the maximum at this stage, allowing the most discriminating comparisons (Souto *et al*., 2006; Giacometti *et al*., 2009).

The vacuolar morphology of strain *tpk1* Δ*/tpk1* Δ *BCY1/bcy1* Δ resembled that previously described in strain *tpk2* Δ*/tpk2* Δ *BCY1/bcy1* Δ (Giacometti *et al*., 2006), with the cytoplasm occupied by a single abnormally large vacuole. Both *tpk* null

DOI: 10.1002/yea

Table 3. Characterization of PKA activity of *tpk1* Δ/*tpk1* Δ *BCY1*/*bcy1* Δ mutant*

Strains	PKA-specific activity pM P incorporated/mg/min		
	Minus cAMP	Plus 10 μM cAMP	Ratio ± cAMP
RGI4	118 ± 0.02	579 ± 0.08	0.2
tpk1 Δ/*tpk1* Δ	96 ± 0.02	480 ± 0.05	0.2
tpk1 Δ/*tpk1* Δ + *BCY1*/*bcy1* Δ	134 ± 0.04	410 ± 0.04	0.32
*tpk2*Δ/*tpk2*Δ	19 ± 0.01	71 ± 0.09	0.26
*tpk2*Δ/*tpk2*Δ *BCY1*/*bcy1* Δ	45 ± 0.07	68 ± 0.1	0.66

* In all strains *URA3* gene was re-established with the Clp10 vector (Murad *et al*., 2000), ensuring *URA3* expression at the neutral *RPS10* locus.

strains harbouring both *BCY1* alleles showed the same vacuolar phenotype as wild-type RGI4 (Figure 1A). The *tpk1* Δ/*tpk1* Δ *BCY1/bcy1* Δ mutant strain exhibited a relatively high PKA-specific activity (Table 3), provided by the more abundant Tpk2p isoform (Cloutier *et al*., 2003; Souto *et al*., 2006), and a low cAMP-binding activity (Figure 1D), which correlated well with a diminished mRNA and Bcy1p expression (Figure 1B, C, E). The fact that cAMP binding of *tpk2* Δ/*tpk2* Δ *bcy1* Δ/*bcy1* Δ strain was negligible reinforces the idea that all binding activity corresponded to the Bcy1p subunit.

The *tpk1* Δ/*tpk1* Δ *BCY1/bcy1* Δ mutant was extremely sensitive to heat exposure (Figure 2, streak 4), due to the presence of the less regulated Tpk2p isoform, which we have reported to be involved in conferring thermosensitivity to the cell (Giacometti *et al*., 2009). Identical results were obtained with three independently isolated clones (data not shown).

We then characterized the ability of *tpk1* Δ/*tpk1* Δ *BCY1/bcy1* Δ mutant strain to shift from yeast to hyphal growth (YPD medium plus 10% FBS at 37 °C) and compared it with previously obtained *BCY1* heterozygous strains (Giacometti *et al*., 2006). The results obtained are shown in Figure 3. Under this hypha-only inducing condition, the wild-type strain exhibited about 90–97% hyphae and 1–3% pseudohyphae. In contrast, we found that the other strains differed in the proportion of pseudohyphae formed. Similarly to other heterozygous *BCY1* mutant strains, *tpk1* Δ/*tpk1* Δ *BCY1/bcy1* Δ produced a mixture of hyphae and pseudohyphae. However, strain *tpk2* Δ/*tpk2* Δ *BCY1/bcy1* Δ exhibited the higher proportion of pseudohyphae; even strain *tpk2* Δ/*tpk2* Δ, harbouring both *BCY1* alleles, also produced a significant amount of pseudohyphae, very probably due to the lower expression of *BCY1* in this strain (Giacometti *et al*., 2009; Souto, PhD Thesis, 2006). Complementation of the *tpk2* Δ/*tpk2* Δ mutant with a wild-type copy of *TPK2* increased the levels of hyphae formation and reduced pseudohyphae proportion, suggesting a key role for Tpk2p in the hyphae/pseudohyphae-forming decision. Although the effect was less noticeable, *tpk1* Δ/*tpk1* Δ mutant restored with a wild-type copy of *TPK1* also reduced the already low levels of pseudohyphae.

A careful observation of cell population revealed considerable differences between the *tpk2* Δ/*tpk2* Δ and *tpk1* Δ/*tpk1* Δ strains. As can be seen in Figure 4A, the pseudohyphae were shorter and exhibited more lateral buds and branches in those strains devoid of *TPK2* alleles. Also, in these strains the number of constrictions per filament increased, while compartment length was diminished (Figure 4B). In contrast, strains harbouring *TPK2*, including complemented *tpk2* Δ/*tpk2* Δ:: *TPK2* strain, showed extended filaments with fewer constrictions. As expected, DAPI staining of pseudohyphae revealed one nucleus per compartment (Figure 4C). The above data showed that under hypha-only inducing conditions low Bcy1p levels promoted the development of pseudohyphae; while absence of Tpk2p impaired pseudohyphae elongation.

Pseudohypha elongation depends on the expression of Tpk2p isoform

In view of the results described above, morphological differences between strains of the whole set were assessed under pseudohyphae-only inducing conditions (YPD medium at 35 °C). Cell morphology was monitored after 2 h. As can be seen in Figure 5A, all strains were able to develop pseudohyphal growth. However, striking differences in cell morphology could be observed. Thus, all strains lacking *TPK2* alleles formed chains of budding yeast cells that remain attached to each other (see strains *tpk2* Δ/*tpk2* Δ, *tpk2* Δ/*tpk2* Δ *TPK1/tpk1* Δ, *tpk2* Δ/*tpk2* Δ *BCY1/bcy1* Δ and *tpk2* Δ/*tpk2* Δ *bcy1* Δ/*bcy1* Δ). The *TPK2/tpk2* Δ

DOI: 10.1002/yea

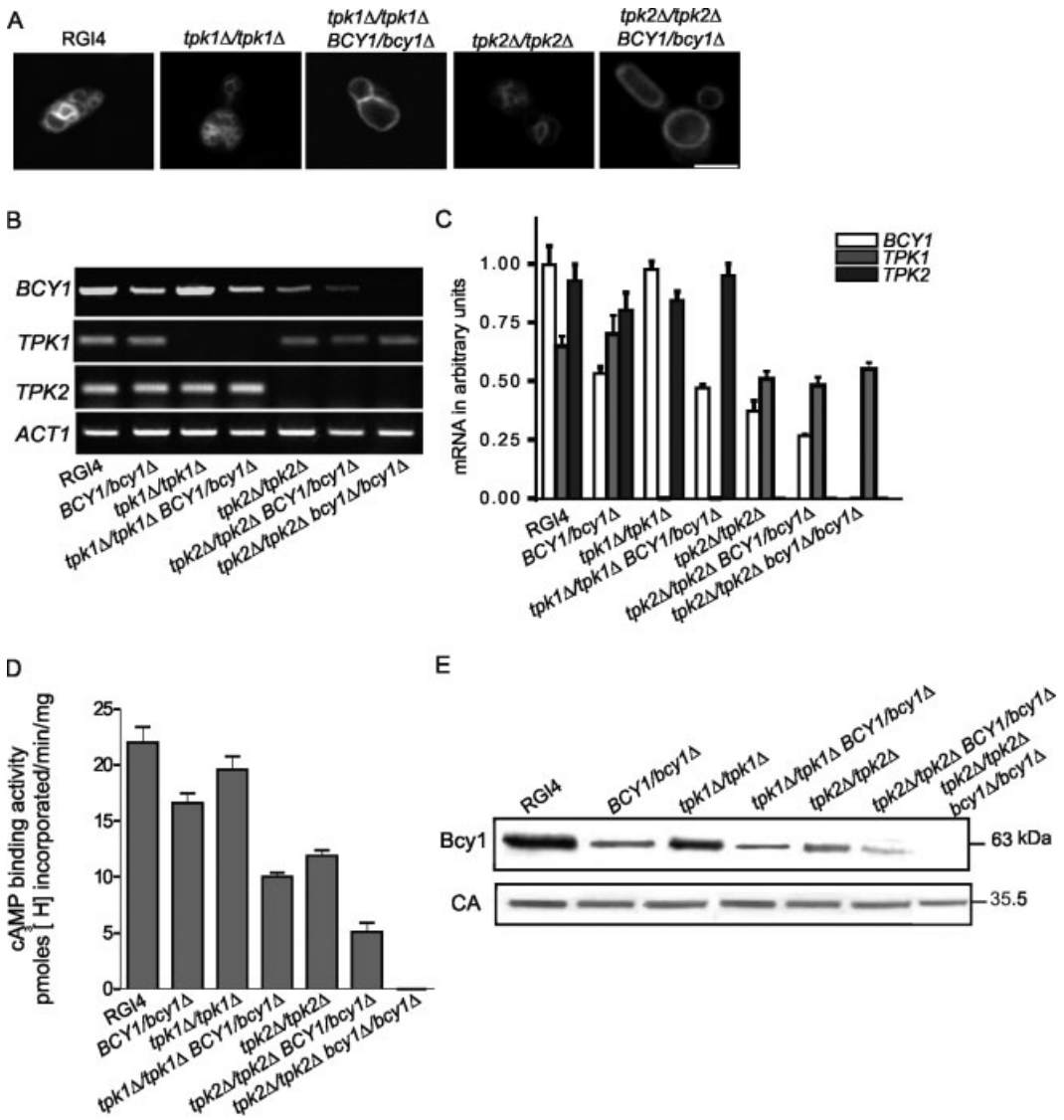

Figure 1. Characterization of strain *tpk1*Δ/*tpk1*Δ *BCY1*/*bcy1*Δ (RG12.1u) in comparison with mutant *tpk1*Δ/*tpk1*Δ (RS1u), *tpk2*Δ/*tpk2*Δ (RS2u), *tpk2*Δ/*tpk2*Δ *BCY1*/*bcy1*Δ (BBA1u), *tpk2*Δ/*tpk2*Δ *bcy1*Δ/*bcy1*Δ (EC1u) and wild-type RGI4. (A) Vacuole staining with the lipophylic dye MDY4-64, scale bar 10 μm. (B) Semi-quantitative RT–PCR analysis of *TPK* and *BCY1* mRNAs; ethidium bromide stained agarose gels to visualize *BCY1, TPK1* and *TPK2* transcripts. (C) RT–PCR data were expressed in arbitrary units and values were normalized to actin (*ACT1*). (D) [^{3}H] cAMP binding activity. (E) Bcy1p levels by Western blot analysis. Soluble extracts from stationary phase cells (1 μg protein) were resolved in a 10% SDS–PAGE, transferred to PVDF membranes and developed with anti-Bcy1p antiserum, as described in Materials and methods. The molecular masses of Bcy1p and carbonic anhydrase (CA) are indicated on the right

strain showed a mixture of long and short pseudohyphae. Complementation of the *tpk2* Δ/*tpk2* Δ mutant with a wild-type copy of *TPK2* restored the elongation capability of pseudohyphae, confirming that Tpk2p was required for elongation of pseudohyphae. In contrast, wild-type, homozygous and heterozygous *tpk1* Δ mutants developed pseudomycelia formed by elongated filaments with fewer compartments between constrictions. The average compartment lengths of the *tpk2* Δ/*tpk2* Δ mutants were approximately 50% shorter than *tpk1* Δ/*tpk1* Δ and wild-type (Figure 5B).

A study by Crampin *et al*. (2005) revealed that different molecular mechanisms drive polarized

DOI: 10.1002/yea

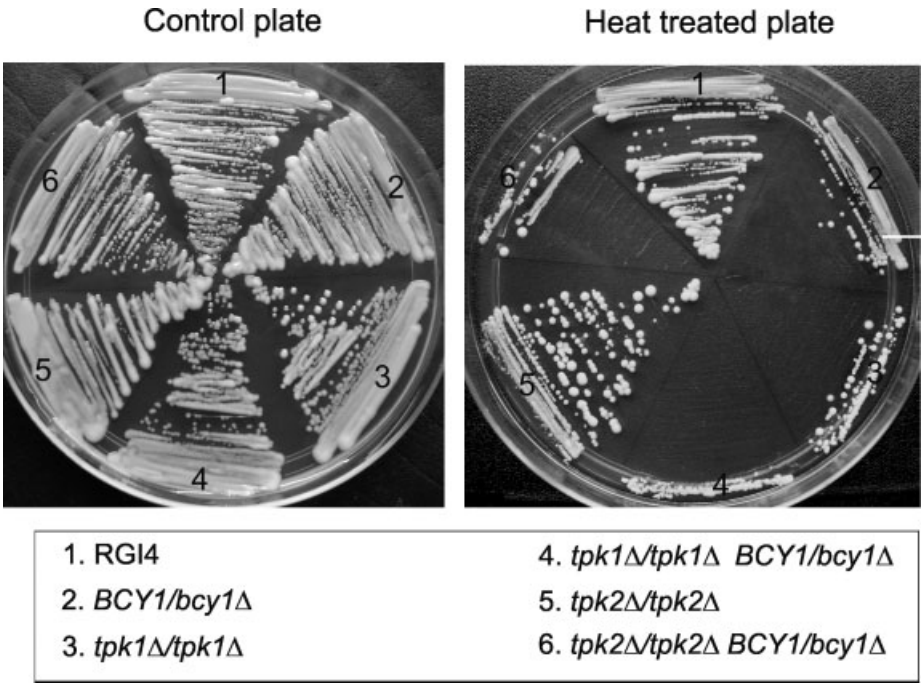

Figure 2. Effect of heat shock on growth of *tpk1* Δ/*tpk1* Δ *BCY1*/*bcy1* Δ mutant. Yeast cells from wild-type RGI4, *BCY1*/*bcy1* Δ (RG65), *tpk1* Δ/*tpk1* Δ (RS1u), *tpk1* Δ/*tpk1* Δ *BCY1*/*bcy1* Δ (RG12.1u), *tpk2*Δ/*tpk2*Δ (RS2u) and *tpk2*Δ/*tpk2*Δ *BCY1*/*bcy1* Δ (BBA1u) mutants from the stationary stage of growth were streaked out on YPD plates. The control plate was incubated at 30 °C (left panel); the heat-shocked plate was held at 50 °C for 2 h and then shifted to 30 °C (right panel). Growth was analysed after 2 days

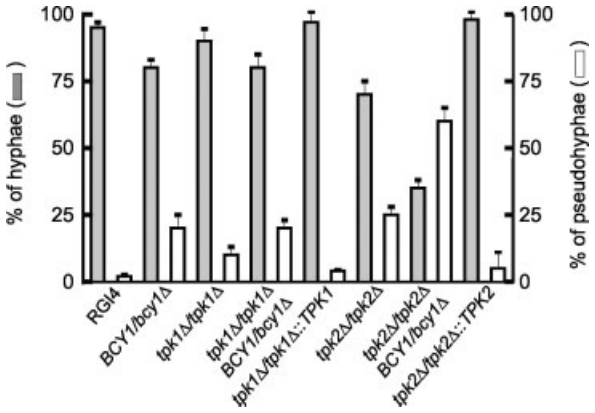

Figure 3. Hyphae and pseudohyphae formation from strains RGI4, *BCY1*/*bcy1* Δ (RG65), *tpk1* Δ/*tpk1* Δ (RS1u), *tpk1* Δ/*tpk1* Δ *BCY1*/*bcy1* Δ (RG12.1u), *tpk1* Δ/*tpk1* Δ::*TPK1* (HPY321), *tpk2*Δ/*tpk2*Δ (RS2u), *tpk2*Δ/*tpk2*Δ *BCY1*/*bcy1* Δ (BBA1u) and *tpk2*Δ/*tpk2*Δ::*TPK2* (HPY421) under hypha-only inducing conditions. Strains were grown in YPD at 30 °C overnight and about 1×10^7 cells were transferred to liquid YPD plus 10% FBS. Cells with hyphae (grey bars) or pseudohyphae (empty bars) were scored as a percentage of the total germinated cells (± SD from three independent experiments). At 2 h post induction 80–90% of the cells had germinated

growth in hyphae as compared to pseudohyphae. Our results indicated that Tpk2p but not Tpk1p played an important role in pseudohypha elongation.

TPK2 deletion results in a disorganized and weakened biofilm structure

It was reported by Bockmühl *et al*. (2001) that *tpk2* Δ/*tpk2* Δ but not *tpk1* Δ/*tpk1* Δ mutants were deficient in invading agar. Also, Park *et al*. (2005) described the reduced capacity of *tpk2* Δ/*tpk2* Δ mutant to invade and damage oral epithelial cells. Furthermore, several reports have shown that filamentation is not strictly required for biofilm formation, but is definitively involved in the complex architecture of the biofilm (Baillie and Douglas, 1999). In view of these facts, we hypothesized that strains lacking the Tpk2p isoform would show an altered biofilm development. Therefore, we quantified biofilm production of *tpk1* Δ/*tpk1* Δ and *tpk2* Δ/*tpk2* Δ strains carrying one or both *BCY1* alleles by the violet crystal assay (Figure 6A, grey bars) and using the XTT reduction method (empty

DOI: 10.1002/yea

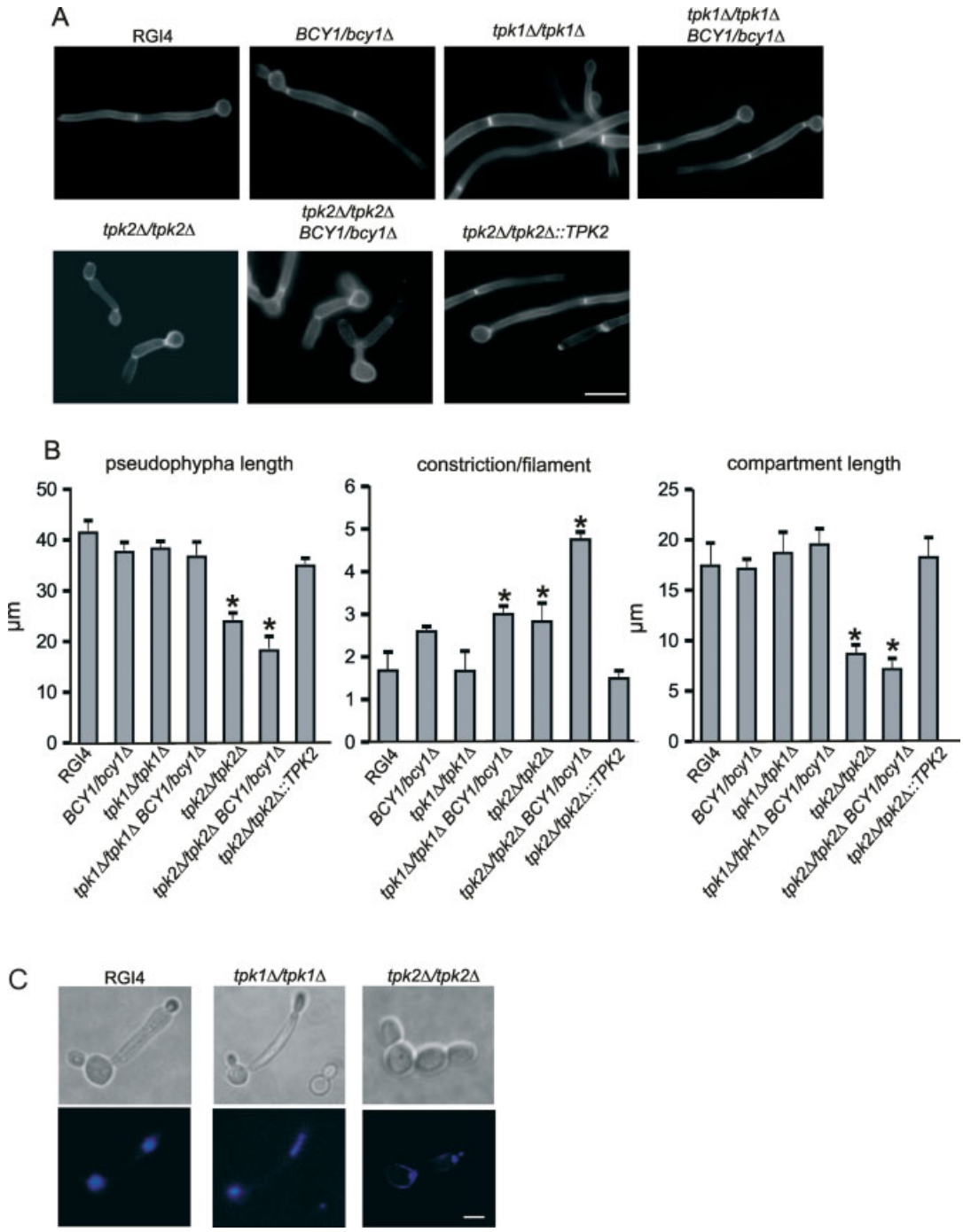

Figure 4. Pseudohyphae characterization of wild-type and PKA mutant strains under hypha-only inducing conditions. RGI4, *BCY1/bcy1*Δ (RG65), *tpk1*Δ/*tpk1*Δ (RS1u), *tpk1*Δ/*tpk1*Δ *BCY1/bcy1*Δ (RG12.1u), *tpk2*Δ/*tpk2*Δ (RS2u), *tpk2*Δ/*tpk2*Δ *BCY1/bcy1*Δ (BBA1u) and *tpk2*Δ/*tpk2*Δ::*TPK2* (HPY421) strains were grown in YPD at 30 °C overnight and about 1×10^7 cells were transferred to liquid YPD plus 10% FBS. (A) Two hours after induction, pseudohyphae were stained with CFW; scale bar = 10 µm. (B) Measurement of pseudohyphae length, number of constrictions per filament and compartment length (µm). $^*p \leq 0.01$. Error bars represent standard error (SE). (C) DAPI staining of RGI4, *tpk1*Δ/*tpk1*Δ (RS1u) and *tpk2*Δ/*tpk2*Δ (RS2u) pseudohyphae; scale bar = 5 µm

DOI: 10.1002/yea

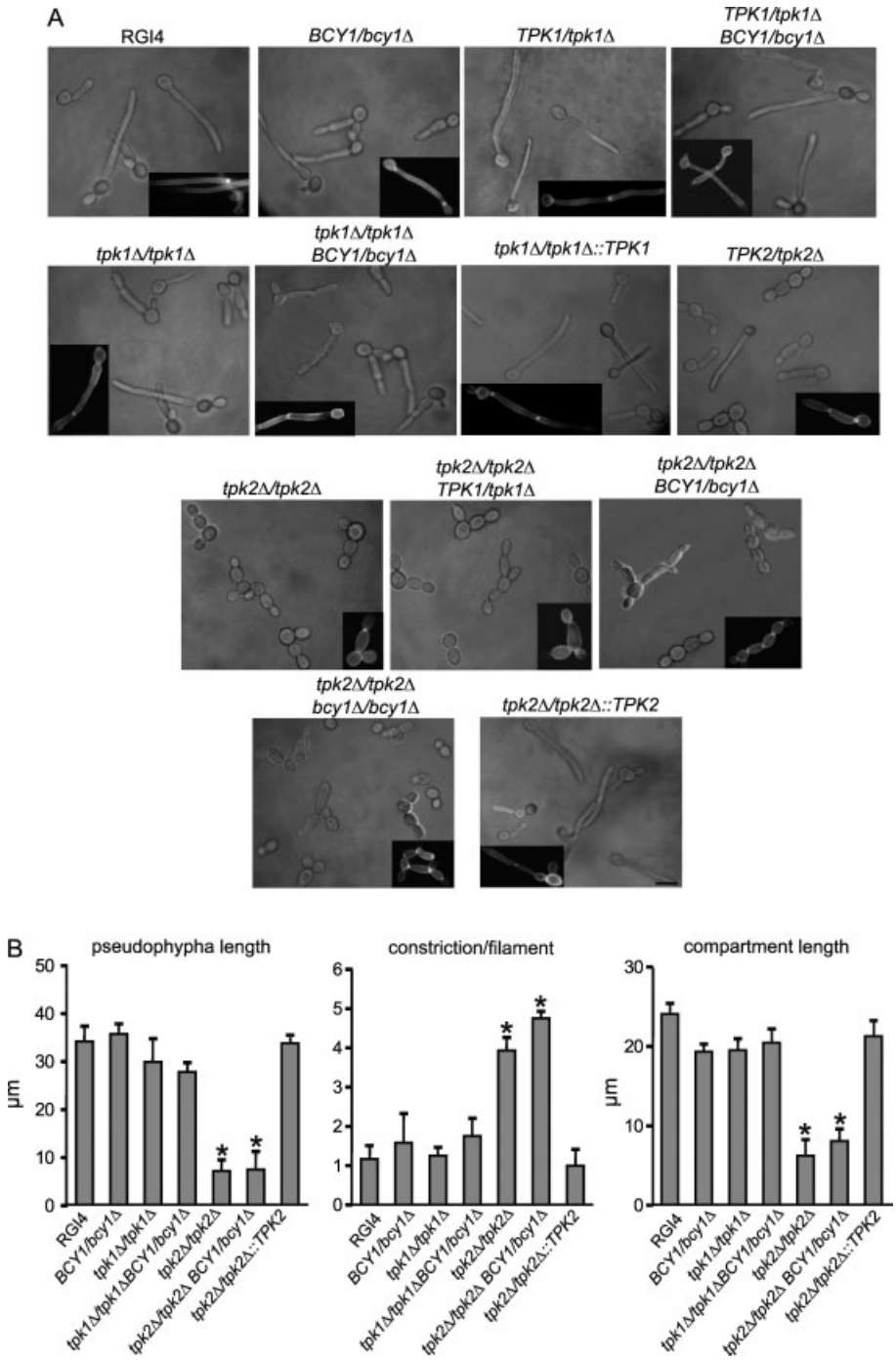

Figure 5. Pseudohyphal germinative behaviour of wild-type and PKA mutant strains. (A) Stationary-phase yeast cells from wild-type RGI4 and mutants *BCY1/bcy1*Δ (RG65), *TPK1/tpk1*Δ (R1U1.1), *TPK1/tpk1*Δ *BCY1/bcy1*Δ (RG11.1), *tpk1*Δ/*tpk1*Δ (RS1u), *tpk1*Δ/*tpk1*Δ *BCY1/bcy1*Δ (RG12.1u), *tpk1*Δ/*tpk1*Δ::*TPK1* (HPY321), *TPK2/tpk2*Δ (R2U2.1), *tpk2*Δ/*tpk2*Δ (RS2u), *tpk2*Δ/*tpk2*Δ *TPK1/tpk1*Δ (RS11u), *tpk2*Δ/*tpk2*Δ *BCY1/bcy1*Δ (BBA1u), *tpk2*Δ/*tpk2*Δ *bcy1*Δ/*bcy1*Δ (EC1u) and *tpk2*Δ/*tpk2*Δ::*TPK2* (HPY421) were induced to germinate for 2 h at 35 °C in fresh YPD medium; scale bar = 10 µm. Insets on the corners show germinated cells stained with CFW. (B) Measurement of pseudohyphae length, number of constrictions per filament and compartment length (µm). $^*p \leq 0.01$. Error bars represent SE

DOI: 10.1002/yea

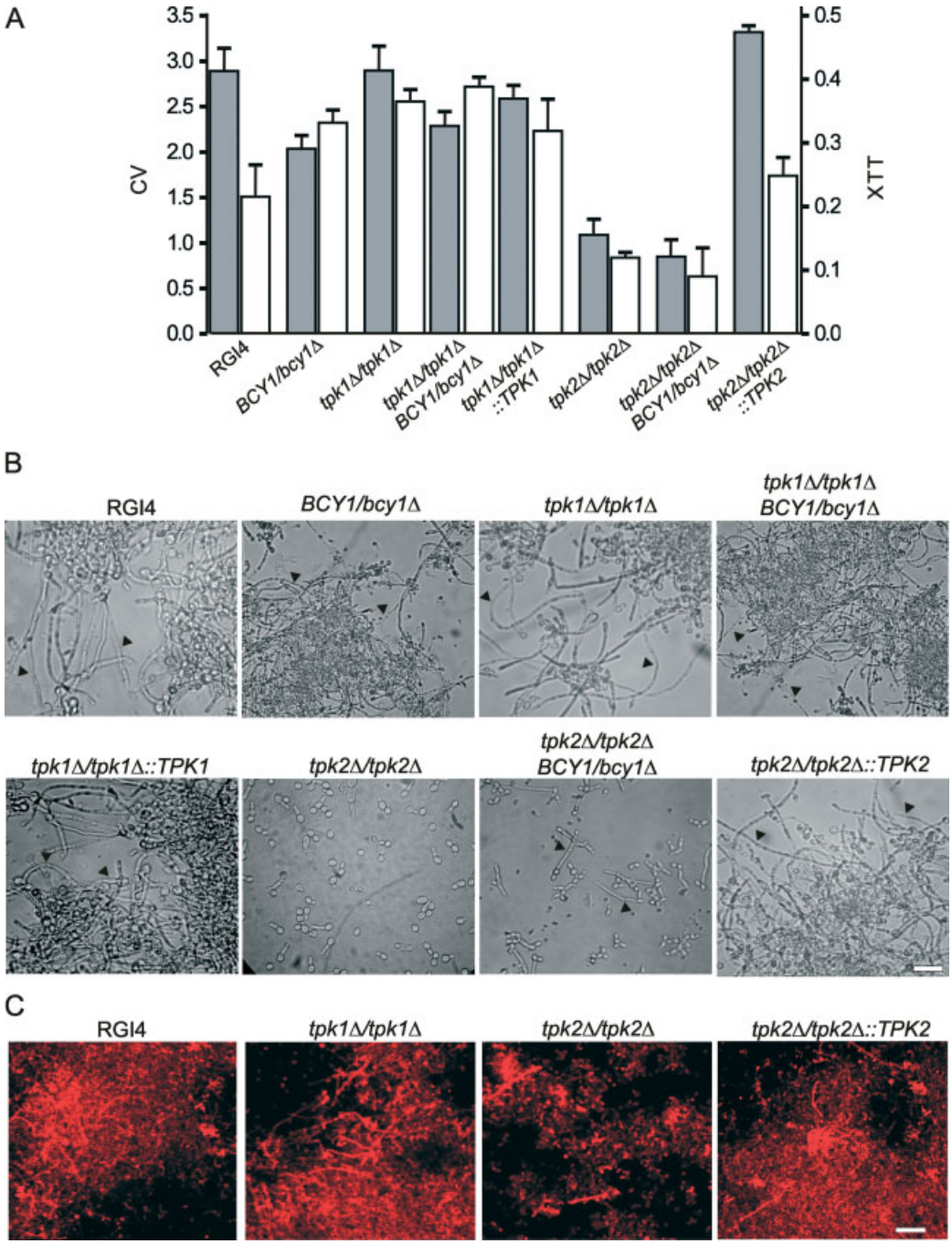

Figure 6. Biofilm formation and metabolic activity in *BCY1/bcy1*Δ (RG65), *tpk1*Δ/*tpk1*Δ (RS1u), *tpk1*Δ/*tpk1*Δ *BCY1/bcy1*Δ (RG12.1u), *tpk1*Δ/*tpk1*Δ::*TPK1* (HPY321), *tpk2*Δ/*tpk2*Δ (RS2u), *tpk2*Δ/*tpk2*Δ *BCY1/bcy1*Δ (BBA1u) and *tpk2*Δ/*tpk2*Δ::*TPK2* (HPY421) in comparison to wild-type RGI4. (A) Biofilm production in 96-well plates was quantified using crystal violet staining (grey bars). Biofilm metabolic activity was quantified using the XTT reduction assay (empty bars). The mean ± SD was determined from three independent experiments, measuring 10 replicates for each strain. (B) Biofilm cell morphology was observed at ×40. Pseudohypha constrictions are indicated by black arrowheads. (C) CSLM of biofilm formed on silicone squares stained with concanavalin A, observed at ×100 water immersion; scale bar = 50 μm

DOI: 10.1002/yea

bars) to quantify metabolic activity. Growth of the *tpk2* Δ/*tpk2* Δ strain resulted in a weakened structure that was obvious immediately when viewing the biofilms in the 96-well plate in which they were grown. The mature biofilm was dislodged easily from the bottom of the well and readily crumbled into many pieces when the 96-well plate was moved from the incubator. The 48 h biofilm mass from *tpk2* Δ/*tpk2* Δ and *tpk2* Δ/*tpk2* Δ *BCY1/bcy1* Δ was significantly less than that of the rest of the strains.

As judged by light microscopy (Figure 6B), the three morphologies were present in biofilms from all strains tested. However, strains *tpk2* Δ/*tpk2* Δ and *tpk2* Δ/*tpk2* Δ *BCY1/bcy1* Δ failed to form highly extended filaments, while strains *BCY1/bcy1* Δ, *tpk1* Δ/*tpk1* Δ, *tpk1* Δ/*tpk1* Δ *BCY1/bcy1* Δ, *tpk1* Δ/*tpk1* Δ::*TPK1* and wild-type strain were able to form mycelia composed of long tubular cells. Strains lacking Tpk2p isoform showed parallel filaments in the mutant biofilm that contrasted in appearance with the intertwining hyphae and pseudohyphae present in the *tpk1* Δ/*tpk1* Δ and in RGI4 biofilm structure. Reintegration of the *TPK2* wild-type allele in strain *tpk2* Δ/*tpk2* Δ restored the production of long filaments similar to those of the reference wild-type strain.

The results described above prompted us to assess the ability of these strains to adhere to an abiotic support, such as squares of silicone catheter material. As can be seen in Figure 6C, images from confocal scanning laser microscopy (CSLM) inspection of silicone slices revealed that the biofilm morphology of *tpk1* Δ/*tpk1* Δ and RGI4 strain was similar, composed of a dense population of predominantly mature filamentous forms. In contrast, in a background of catalytic activity provided exclusively by Tpk1p, the biofilm formed was markedly less dense, composed of short pseudohyphae, few true hyphae and yeast cells (see mutant *tpk2* Δ/*tpk2* Δ). Reconstitution of the *TPK2* wild-type allele in strain *tpk2* Δ/*tpk2* Δ restored biofilm architecture and adhesion ability. The fragile biofilm formed by the *tpk2* Δ/*tpk2* Δ strain could be the consequence of the morphological abnormalities observed under conditions promoting hyphae and pseudohyphae.

The filamentation and adherence defects for *tpk2* Δ/*tpk2* Δ strain are in agreement with the reduction in virulence of *tpk2* null strain in a mouse intravenous and mouse oropharyngeal infection model *in vitro* (Park *et al*., 2005). These findings suggested a significant defect in cell adherence of *tpk2* Δ/*tpk2* Δ strains, very probably due to a different expression pattern of genes involved in cell–cell interaction, such as adhesins, and/or cell to surface adhesion.

Adhesins Als1p and Als3p are poorly expressed in a *tpk2*-null background

In *S. cerevisiae*, filamentation and cell aggregation are both subjected to regulatory pathways that converge on Flo11p, an effector of flocculation. Different pathways are known to regulate the expression of *FLO* genes in yeast, among them the Ras1-cAMP signalling cascade (Verstrepen and Klis, 2006). Downstream, Tpk2p activates Flo8p and represses Sfl1p, which encodes a suppressor of flocculation (Conlan and Tzamarias, 2001). Sfl1p is regulated by Tpk2p phosphorylation (Robertson and Fink, 1998).

In *C. albicans, ALS* genes encode a family of cell-surface glycoproteins, some of which control adhesion to host surfaces (reviewed in Hoyer *et al*., 2008). It has been shown that the expression of Als1p and Als3p, both effectors of filamentation, function redundantly to promote biofilm formation (Nobile *et al*., 2008) and are also controlled by the transcription factor Efg1p (Fu *et al*., 2002; Zhao *et al*., 2004), which in turn is believed to be regulated by Tpk2p (Lengeler *et al*., 2000; Sonneborn *et al*., 2000).

Since adhesion to surfaces and cell–cell interaction are closely related, it was of interest to assess the ability of Tpk1p and Tpk2p isoforms to mediate flocculation (see Figure 7). When grown as blastospores in SD minimal liquid medium, the decreased degree of clumping in the *tpk2* Δ/*tpk2* Δ mutant was dramatic (Figure 7A). Under the hypha-inducing condition, wild-type RGI4, *tpk1* Δ/*tpk1* Δ and reintegrated *tpk2* Δ/*tpk2* Δ::*TPK2* strain flocculated extensively, forming large aggregates of cells that rapidly sedimented to the bottom of the tube; while the *tpk2* Δ/*tpk2* Δ mutant flocculated minimally under this condition (Figure 7A, B).

In view of the described defect in flocculation of the *tpk2* null strain, we investigated the cell surface localization of Als1p and Als3p adhesins, using indirect immunofluorescence with anti-Als1p and anti-Als3p monoclonal antibodies (see Figure 8).

DOI: 10.1002/yea

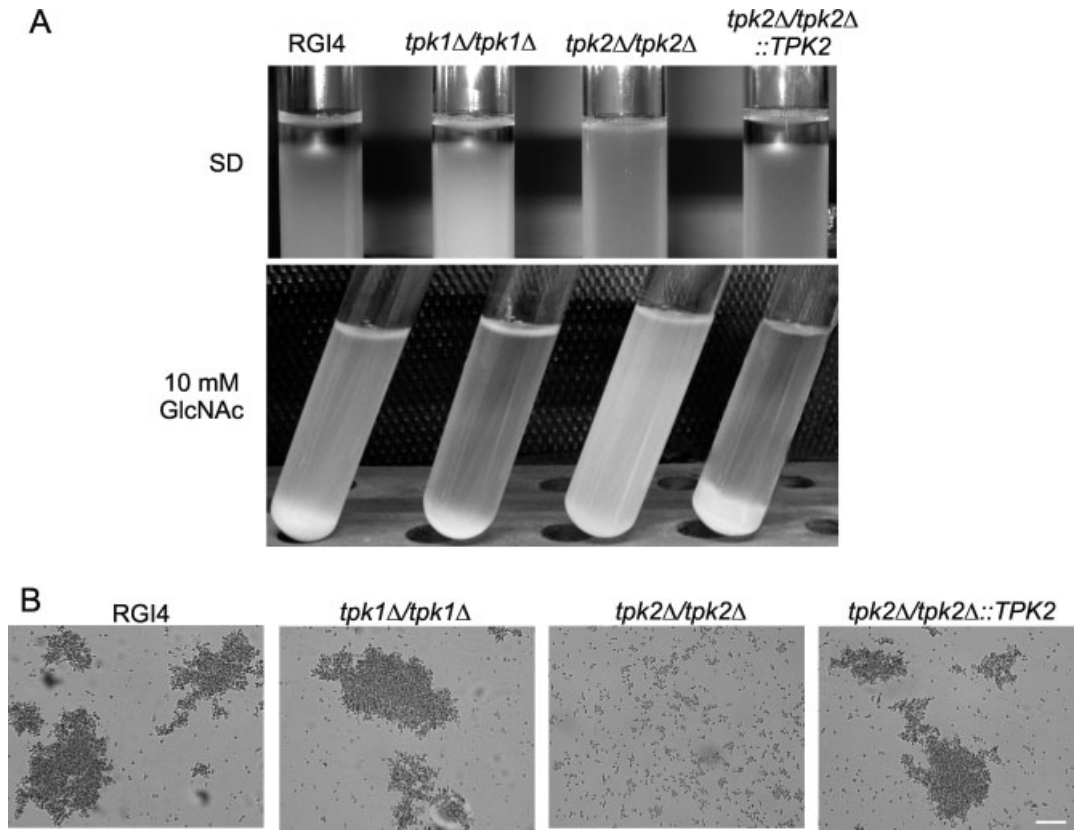

Figure 7. Flocculation assessment of RGI4, *tpk1*Δ/*tpk1*Δ (RS1u), *tpk2*Δ/*tpk2*Δ (RS2u) and *tpk2*Δ/*tpk2*Δ::*TPK2* strains (HPY421). The strains were grown overnight in SD liquid medium at 30 °C or in Shepherd medium plus 10 mM GlcNAc at 37 °C for 2 h. Images of tubes containing cells in media (A) and microscopic images from germinated cells (B) are shown; scale bar = 10 μm

As can be seen, a faint staining for both proteins was detected on the surface of *tpk2* Δ/*tpk2* Δ germ tubes after 1 h of growth in YPD plus 10% FBS. This staining was more intense on the hyphae surface of wild-type, *tpk1* Δ/*tpk1* Δ and reintegrated *tpk2* Δ/*tpk2* Δ::*TPK2* strains. In these strains occasional areas of brighter staining were observed at the hyphal tip. No immunofluorescence was observed in blastospores or in pseudohyphae from wild-type or *tpk* mutants (not shown). Although the above results are only qualitative, they suggest that isoform Tpk2p is predominately controlling cell aggregation. Considering that *EFG1* is regulated by Tpk2p (Lengeler *et al*., 2000; Sonneborn *et al*., 2000) and that *efg1* null mutants failed to express *ALS1* (Fu *et al*., 2002), it is reasonable to assume that in *tpk2* Δ/*tpk2* Δ strain Efg1p is less activated and consequently Als proteins are poorly expressed. These results are in line with those of Nobile *et al*. (2006), who found that a null mutant of the transcription factor *BCR1* exhibited a reduced expression of both *ALS1* and *ALS3*, which seems to be critical for its biofilm defect.

Our recent genetic and biochemical studies of PKA mutants allowed us to uncover several Tpk functional specificities. Thus, in a previous report we showed that Tpk1p and Tpk2p, despite a high level of amino acid sequence identity and overlapping roles in viability, are not redundant in stress and glycogen metabolism (Giacometti *et al*., 2009). The results presented here further indicate that Tpk2p plays a major role in regulating pseudohyphal filament extension, biofilm formation and cell adherence.

A more detailed understanding of these regulatory mechanisms will no doubt allow us to gain broader insight into the relationship between fungal morphology and virulence.

DOI: 10.1002/yea

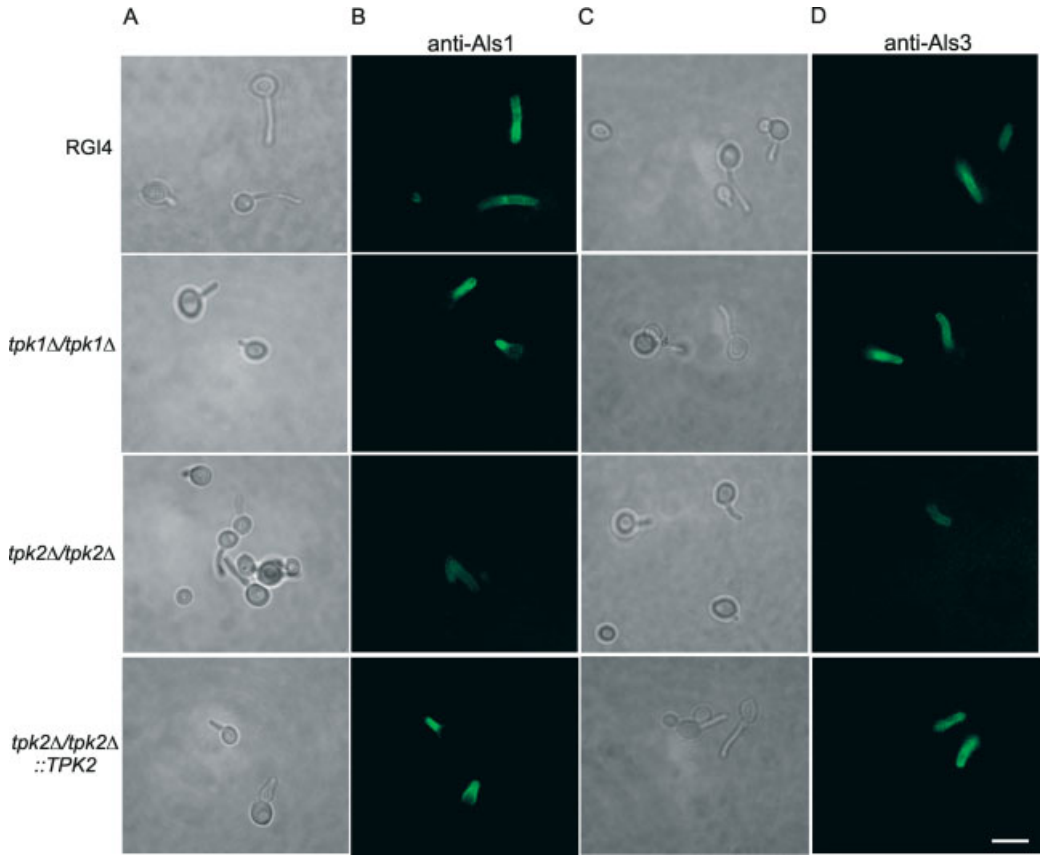

Figure 8. *C. albicans* cells from strains RGI4, *tpk1*Δ/*tpk1*Δ (RS1u), *tpk2*Δ/*tpk2*Δ (RS2u) and *tpk2*Δ/*tpk2*Δ::*TPK2* (HPY421) labelled with either anti-Als1 or anti-Als3 MAb and Alexa Fluor 488 conjugated secondary antibody. (B) Als1p detection through CSLM of the surface of germ tubes grown in YPD + 10% FBS for 1 h. Als3p detection is shown in (D). (A, C) The same images as (B) and (D), respectively, illuminated with white light only. Scale bar = 10 μm

Acknowledgements

We thank Dr Hyunsook Park for kindly providing the HPY421 and HPY321 strains, Dr Lois Hoyer for her kind donation of anti-Als1 and Als3 MAb, and Dr Dana Davis for the fluorescent antibody Alexa Fluor 488. We also thank Dr Eduardo Passeron and Dr Lucia Zacchi for critical reading of the manuscript. This work was supported by grants from the Consejo Nacional de Investigaciones Científicas y Técnicas (CONICET) and Agencia Nacional de Promoción Científica y Tecnológica (ANPCyT) to S.P. and by the Europrofession Foundation (Saarbrücken) and the BMBF Go-Bio programme to R.M.B.

References

Abramoff MD, Magelhaes PJ, Ram SJ. 2004. Image processing with ImageJ. *Biophotonics Int* **11**: 36–42.

Adams A, Gottschling DE, Kaiser CA, Stearns T. 1997. *Techniques and Methods in Yeast Genetics*, Dickerson MM (ed.). Cold Spring Harbor Laboratory Press: Cold Spring Harbor, NY; 99–102.

Ausubel FM, Brent R Kingston RE, *et al*. 1994. *Current Protocols in Molecular Biology*, Chanda VB (ed.). Wiley: New York.

Baillie GS, Abramoff MD, Magelhaes PJ, Ram SJ. 2004. Image processing with ImageJ. *Biophotonics Int* **11**: 36–42.

Bockmühl DP, Krishnamurthy S, Gerards M, *et al*. 2001. Distinct and redundant roles of the two protein kinase A isoforms Tpk1p and Tpk2p in morphogenesis and growth of *Candida albicans*. *Mol Microbiol* **42**: 1243–1257.

Brand A, MacCallum DM, Brown AJ, *et al*. 2004. Ectopic expression of *URA3* can influence the virulence phenotypes and proteome of *Candida albicans* but can be overcome by targeted reintegration of *URA3* at the *RPS10* locus. *Eukaryot Cell* **3**: 900–909.

Braun BR, Head WS, Wang MX, Johnson AD. 2000. Identification and characterization of TUP1-regulated genes in *Candida albicans*. *Genetics* **156**: 31–44.

Carlisle PL, Banerjee M, Lazzell A, *et al*. 2009. Expression levels of a filament-specific transcriptional regulator are sufficient to determine *Candida albicans* morphology and virulence. *Proc Natl Acad Sci USA* **106**: 599–604.

Cassola A, Parrot M, Silberstein S, *et al*. 2004. *Candida albicans* lacking the gene encoding the regulatory subunit of the cAMP-dependent protein kinase displays a defect in hyphal formation and an altered localization of the catalytic subunit. *Eukaryot Cell* **3**: 190–199.

Chandra JD, Kuhn M, Mukherjee PK, *et al*. 2001. Biofilm formation by the pathogen *C. albicans* — development, architecture, and drug resistance. *J Bacteriol* **183**: 5385–5394.

Cloutier M, Castilla R, Bolduc N, *et al*. 2003. The two isoforms of the cAMP-dependent protein kinase catalytic subunit are involved in the control of dimorphism in the human fungal pathogen *Candida albicans*. *Fungal Genet Biol* **38**: 133–141.

Cole L, Orlovich DA, Ashford AE. 1998. Structure, function, and motility of vacuoles in filamentous fungi. *Fungal Genet Biol* **24**: 86–100.

Conlan RS, Tzamarias D. 2001. Sfl1 functions via the co-repressor Ssn6-Tup1 and the cAMP-dependent protein kinase Tpk2. *J Mol Biol* **309**: 1007–1015.

Crampin H, Finley K, Gerami-Nejad M, *et al*. 2005. *Candida albicans* hyphae have a Spitzenkörper that is distinct from the polarisome found in yeast and pseudohyphae. *J Cell Sci* **118**: 2935–2947.

Fonzi WA, Irwin MY. 1993. Isogenic strain construction and gene mapping in *Candida albicans*. *Genetics* **134**: 717–728.

Fu Y, Ibrahim AS, Sheppard DC, *et al*. 2002. *Candida albicans* Als1p: an adhesin that is a downstream effector of the *EFG1* filamentation pathway. *Mol Microbiol* **44**: 61–72.

Giacometti R, Kronberg F, Biondi RM, Passeron S. 2009. Roles of *Candida albicans* PKA catalytic isoforms Tpk1 and Tpk2 in stress response, nutrient deprivation and glycogen content. *Yeast* **26**: 273–285.

Giacometti R, Souto G, Silberstein S, *et al*. 2006. Expression levels and subcelullar localization of Bcy1p in *Candida albicans* mutant strains devoid of one *BCY1* allele results in a defective morphogenetic behavior. *Biochim Biophys Acta* **1763**: 64–72.

James TY, Kauff F, Schoch CL, *et al*. 2006. Reconstructing the early evolution of fungi using a six-gene phylogeny. *Nature* **443**: 819–822.

Jung WH, Stateva L. 2003. The cAMP phosphodiesterase encoded by Ca*PDE2* is required for hyphal development in *Candida albicans*. *Microbiology* **149**: 2961–2976.

Kuhn DM, Chandra J, Mukherjee PK, Ghannoum MA. 2002. Comparison of biofilms formed by *Candida albicans* and *Candida parapsilosis* on bioprosthetic surfaces. *Infect Immun* **70**: 878–888.

Li WJ, Wang YM, Zheng XD, *et al*. 2006. The F-box protein Grr1 regulates the stability of Ccn1, Cln3 and Hof1 and cell morphogenesis in *Candida albicans*. *Mol Microbiol* **62**: 212–226.

Liu H, Köhler J, Fink GR. 1994. Suppression of hyphal formation in *Candida albicans* by mutation of a *STE12* homolog. *Science* **266**: 1723–1725.

Lowry OH, Rosebrough NJ, Farr A, Randall RJ. 1951. Protein measurements with the phenol reagent. *J Biol Chem* **193**: 265–275.

Murad AM, Lee PR, Broadbent ID, *et al*. 2000. CIp10, an efficient and convenient integrating vector for *Candida albicans*. *Yeast* **16**: 325–327.

Nobile CJ, Andes DR, Nett JE, *et al*. 2006. Critical role of Bcr1-dependent adhesins in *C. albicans* biofilm formation *in vitro* and *in vivo*. *PLoS Pathog* **2**: e63.

Nobile CJ, Schneider HA, Nett JE, *et al*. 2008. Complementary adhesin function in *C. albicans* biofilm formation. *Curr Biol* **18**: 1017–1024.

Odds FC. 1988. *Candida and Candidiasis*, 2nd edn. Baillière Tindall: London.

Park H, Myers CL, Sheppard DC, *et al*. 2005. Role of the fungal Ras protein kinase A pathway in governing epithelial cell interactions during oropharyngeal candidiasis. *Cell Microbiol* **7**: 499–510.

Ptacek J, Devgan G, Michaud G, *et al*. 2005. Global analysis of protein phosphorylation in yeast. *Nature* **438**: 679–684.

Robertson LS, Fink GR. 1998. The three yeast A kinases have specific signaling functions in pseudohyphal growth. *Proc Natl Acad Sci USA* **95**: 13783–13787.

Sambrook J, Fritsch EF, Maniatis T. 1989. *Molecular Cloning: A Laboratory Manual*. Cold Spring Harbor Laboratory Press: Cold Spring Harbor, New York.

Sherman F, Fink GR, Hicks JB. 1986. *Methods in Yeast Genetics*. Cold Spring Harbor Laboratory Press: Cold Spring Harbor, NY.

Sherwood RK, Bennett RJ. 2008. Microtubule motor protein Kar3 is required for normal mitotic division and morphogenesis in *Candida albicans*. *Eukaryot Cell* **7**: 1460–1474.

Souto G. 2006. PhD Thesis, University of Buenos Aires.

Staab JF, Bahn YS, Sundstrom P. 2003. Integrative, multifunctional plasmids for hypha-specific or constitutive expression of green fluorescent protein in *Candida albicans*. *Microbiology* **149**: 2977–2986.

Stoldt VR, Sonneborn A, Leuker CE, Ernst JF. 1997. Efg1p, an essential regulator of morphogenesis of the human fungal pathogen *Candida albicans*, is a member of a conserved class of bHLH proteins regulating morphogenetic processes in fungi. *EMBO J* **16**: 1982–1991.

Sudbery P, Gow NAR, Berman J. 2004. The distinct morphogenic states of *Candida albicans*. *Mol Microbiol* **41**: 19–31.

Sudbery PE. 2001. The germ tubes of *Candida albicans* hyphae and pseudohyphae show different patterns of septin ring localization. *Trends Microbiol* **12**: 317–324.

Tebarth B, Doedt T, Krishnamurthy S, *et al*. 2003. Adaptation of the Efg1p morphogenetic pathway in *Candida albicans* by negative autoregulation and PKA-dependent repression of the *EFG1* gene. *J Mol Biol* **329**: 949–962.

Trunk K, Gendron P, Nantel A, *et al*. 2009. Depletion of the cullin Cdc53p induces morphogenetic changes in *Candida albicans*. *Eukaryot Cell* **8**: 756–767.

Verstrepen KJ, Klis FM. 2006. Flocculation, adhesion and biofilm formation in yeasts. *Mol Microbiol* **60**: 5–15.

Wilson B, Davis D, Mitchell A. 1999. Rapid hypothesis testing with *Candida albicans* through gene disruption with short homology regions. *J Bacteriol* **181**: 1868–1874.

Zelada A, Passeron S, Lopez Gomes S, Cantore ML. 1998. Isolation and characterization of cAMP-dependent protein kinase from *Candida albicans*; purification of the regulatory and catalytic subunits. *Eur J Biochem* **252**: 245–252.

Zhao X, Oh SH, Cheng G, *et al*. 2004. *ALS3* and *ALS8* represent a single locus that encodes a *Candida albicans* adhesin; functional comparisons between Als3p and Als1p. *Microbiology* **150**: 2415–2428.